The Importance of Three-Dimensional Solar Radiative Transfer in Small Cumulus Cloud Fields Derived from the NAURU MMCR and MWR

K. F. Evans and S. A. McFarlane
University of Colorado
Boulder, Colorado

W. J. Wiscombe
National Aeronautics and Space Administration
Goddard Space Flight Center
Greenbelt, Maryland

Introduction

The radiative effects of cloud horizontal inhomogeneity may be divided into two parts (e.g., Varnai and Davies 1999): 1) the one-dimensional heterogeneity effect due to optical depth variability, and 2) the horizontal transport effect of light moving between columns. For climate applications in which domain averaged fluxes are important, the independent pixel approximation (IPA) correctly addresses the first effect, but not the second. There is evidence (Cahalan et al. 1994; Barker et al. 1998) that the IPA accurately predicts domain average solar fluxes in stratocumulus and even cumulus cloud fields. However, it is well known from previous Monte Carlo simulations of finite clouds (e.g., Welch and Wielicki 1984) that there can be large errors in the plane-parallel and independent pixel approximations due to leakage from cloud sides and side illumination of finite clouds. However, there remains the question of how important these three-dimensional (3D) effects are in actual cloud fields. Is the independent pixel approximation adequate to predict domain average solar fluxes and heating rates?

To address this question we need a long term dataset of many observed 3D cloud fields, specifically for cumulus clouds which would be expected to have finite cloud effects. Many individual fields are required so the dataset is statistically representative of a particular location and cloud class, and hence gives a reliable estimate of the actual 3D radiative effects. The Atmospheric Radiation Measurement (ARM) program Millimeter wavelength Cloud Radar (MMCR) and Microwave Radiometer (MWR) datasets are a good source of long term cloud structure information. Nauru is the preferred site for its high frequency of cumulus clouds, its representativeness of a larger region, and to avoid the insect radar contamination problem in Oklahoma. There are considerable difficulties in retrieving cloud extinction from ARM remote sensing datasets, and in converting the retrieved time-height cross sections to 3D cloud fields. This study uses a new Bayesian algorithm to retrieve cloud liquid water and effective radius fields from MMCR and MWR datasets (McFarlane et al. 2001b). We make the simple frozen turbulence assumption with advection speed from a 915 MHz wind profiler to convert the time series to along-wind structure. We have developed a stochastic cloud model to generate random 3D cloud fields

from statistics of observed 2D fields. The purpose of this "data generalization" stochastic model is to create 3D cloud fields that represent the statistics of the input 2D fields as faithfully as possible, not as simply as possible.

Nonprecipitating cumulus cloud field statistics derived from 3 months of Nauru MMCR and MWR data are used to generate 2D and 3D stochastic fields of liquid water content (LWC) and effective radius (r[eff]). Broadband solar radiative transfer is simulated in the observed 2D cloud fields and the stochastic 2D and 3D cloud fields. The effect of cumulus clouds on the reflected and absorbed solar flux (cloud radiative forcing) and the size of the 1D heterogeneity and horizontal transport effects is determined.

Stochastic Cloud Field Generation Method

A stochastic field generation algorithm can generate many random realizations of cloud fields using input statistics derived from data. Here the two horizontal directions are assumed to be equivalent (horizontal isotropy), so that 3D fields may be generated from statistics obtained from 2D radar derived fields. The statistics are assumed to not depend on horizontal location (translational invariance), but do depend on height. It is straightforward to produce fields having the correct single point statistics (probability density function or PDF) for each vertical level. It is much more difficult to generate fields having the desired two-point and higher order statistics, which determine the spatial structure. One method for including partial two-point statistical information is to use Fourier filtering techniques to match the vertical and horizontal correlation function. Fourier filtering techniques have been used in the past to simulate cloud fields in simple stochastic models (e.g., Barker and Davies 1992).

While cloud fields are not gaussian, methods exist to generate gaussian fields with any desired correlation function. These methods can be used as a starting point for a stochastic cloud field generation algorithm. Gaussian fields are completely described by the mean, variance, and correlation function. Since the statistics are assumed to depend on vertical location, but not horizontal location, a cross-correlation matrix, $R^{(i,j)(x)}$, with vertical levels i and j and horizontal separation distance x, describes the spatial structure of a field. The procedure for generating stochastic fields with cross-correlation matrix $R^{(i,j)(x)}$ involves Fourier transforming each element of R to obtain the cross-spectral density matrix, $S^{(i,j)(k)}$. As part of the isotropy assumption, $R^{(i,j)(x)}$ is assumed to be symmetric in x, and thus $S^{(i,j)(k)}$ is real and symmetric in k. For each discrete wavenumber k in Fourier space the eigenvalues and eigenvectors of $S^{(i,j)(k)}$ are calculated. The amplitudes used in the Fourier filtering are the square root of the eigenvalues (or variances). For generating 3D fields from the 2D statistics, the amplitudes are divided by sqrt(k) so that the power spectral density is preserved. A stochastic gaussian field is generated by multiplying independent gaussian random noise by the amplitude for each wavenumber and eigenvalue. The noise vector is then multiplied by the eigenvector matrix for each k to generate vertical vectors of random Fourier components. These vectors are then Fourier transformed for each level to obtain the desired gaussian field. The amplitudes are normalized so that the resulting gaussian field is statistically zero mean and unit variance. The vector Fourier filtering method is closely related to Empirical Orthogonal Functions (EOFs), since EOFs are the eigenvectors of the correlation matrix and the EOFs of a correlation matrix with translational invariance are sines and cosines.

The cloud liquid water content field is highly non-gaussian. Not only is the LWC distribution usually close to log-normal, but over 90 percent of the cumulus field has a LWC of zero (clear sky). It is not difficult, however, to transform a gaussian field to one having the observed LWC histogram using a lookup table. The problem is that doing this nonlinear transformation changes the correlation function so it no longer matches the observed one. Therefore, we need to find the correlation function of the gaussian field ("gaussian correlations") such that when a gaussian field is nonlinearly transformed, the resulting correlation function matches the observed correlations. The simplest method to do this would be to transform the input fields to have a gaussian distribution and then compute the correlation function. This is impossible, however, because the huge lump of probability at zero prevents the LWC distribution from being transformed to a smooth gaussian distribution. There are iterative methods that adjust the gaussian-space power spectrum so that the correct power spectrum is obtained after the nonlinear transformation (e.g., Popescu et al. 1997).

Another approach is to transform the correlation function in the original cloud field space to the equivalent gaussian correlation function. The correlation function of the LWC field describes only a small part of the full two-point statistics. Therefore, we choose instead to match the correlation function of the binary cloud mask field, since the location of the cloud boundaries appears to be important for finite cloud 3D radiative transfer effects. The two-point statistics of a binary field are completely described by its correlation function. Each input time-height LWC field is first linearly interpolated with the advection speed to a horizontal distance grid having the same spacing as the vertical grid. The X-Z LWC field is then thresholded to make a binary field. The cross-covariance matrix as a function of two height levels and lag (i,j,z) is calculated from the binary field using fast Fourier transforms. The cross-covariance matrices for each input field are accumulated and then normalized to produce the binary field cross-correlation matrix $R^{(b)(ij)(x)}$.

The binary field correlations are converted to the gaussian correlations using a lookup table for each pair of levels (i,j). The binary correlation corresponding to a particular gaussian correlation is found with a 2D numerical integration over the bivariate gaussian pdf. The binary correlation depends on the gaussian correlation and the two cloud fractions, and hence depends on the level pair i,j. Unfortunately, the gaussian correlation matrix produced by element-by-element transformation is not positive definite, and hence not a valid correlation matrix. Fundamentally, this is because the elements of a correlation matrix are not independent: if A is highly correlated with B, and B with C, then A and C must be correlated. An optimization procedure is used to find a positive definite correlation matrix that is close to the desired gaussian correlation matrix. The elements of the Cholesky decomposition of the cross-spectral density matrix $S^{(ij)(k)}$ are adjusted to minimize the weighted squared error in the gaussian correlations (with correlations near 1 having more weight). The Cholesky decomposition H is the "square root" of S ($S=H\cdot H^T$), thus the cross-spectral density matrix is guaranteed to be positive definite and so is the correlation matrix $R^{(i,j)(x)}$ (which is the cosine transform of S).

Once the gaussian correlation matrix $R^{(i,j)(x)}$ is calculated, any number of stochastic fields may be generated. The stochastic gaussian fields are computed as described above and then transformed to have the correct LWC distribution with a lookup table for each vertical level. The fields in a whole ensemble, not each output field, are forced to have the observed single point statistics. Since the correlation statistics used in the cloud generation algorithm are based on the cloud boundaries, the same correlation function is used to generate the effective radius (r [eff]) fields. The gaussian noise used to generate the

r[eff] field is correlated with the LWC gaussian noise so that the resulting LWC and r(eff) fields have the observed correlation. The lookup table that converts the gaussian fields to the r(eff) fields is derived from the input fields and depends on the height level and the LWC value. This assures that appropriate values of r(eff) are produced for each LWC value, so that, for example, r(eff)=0 doesn't occur inside of clouds. The resulting stochastic fields should have the correct histogram of LWC and r(eff) for each vertical level and have the observed cross-correlation function for the binary cloud mask field.

Stochastic Cumulus Fields for Nauru

The time-height fields of liquid water content and effective radius are retrieved from MMCR and MWR data using a Bayesian algorithm. A brief description of the algorithm is given in an ARM extended abstract (McFarlane et al. 2001a) and a complete description is provided in a submitted journal article (McFarlane et al. 2001b). Bayes theorem is used to combine the MMCR and MWR measurements, modeled with radiative transfer, with a priori information about the cloud physics of small tropical cumulus. The prior information is derived from droplet size distributions obtained by FSSP and 260X cloud probes flown on aircraft during experiments in Florida and Hawaii. The prior probability distribution is a sum of two trivariate log-normal distributions of the second, third, and sixth moments of the droplet size distribution. The sixth moment is proportional to radar reflectivity, while the second and third moments are directly related to the retrieved LWC and r[eff]. The LWC and r[eff] profiles are retrieved with a Monte Carlo integration over the Bayes theorem posterior pdf. Given the unconstrained nature of the retrieval, much of the retrieval information is derived from the prior pdf and the associated error bars calculated from the posterior pdf are relatively large.

Cloud retrievals are performed for 92 days (June to August, 1999) from the ARM site on Nauru. Of the nearly 795,000 ten-second columns, 33 percent have liquid clouds, but 4 percent are considered raining (mainly by having radar reflectivity above 0 dBZ) and are not retrieved. For input to the stochastic cloud generation, nonraining segments with a minimum length of 1.5 hours are extracted from the 3-hour retrieval periods. There are 623 of these segments, which range from 540 - 1080 columns in length. The 50 range gates with an altitude range of 460 - 2710 m, which contain nearly all the nonprecipitating cumulus clouds, are extracted.

Advection speeds for the cloud fields are obtained from the National Oceanic and Atmospheric Administration (NOAA) 915 MHz wind profiler based at the Nauru airport about 3 km south of the ARM site. The 100 m vertical resolution wind profiles are averaged to the 3-hour periods of the cloud retrievals. The mean LWC profile weighted wind speed for each segment is the single advection speed used to convert time to horizontal distance. The horizontal-to-vertical aspect ratio of the retrieved pixels ranges from 0.56 - 3.2 and averages 1.9 (8.6 m/s x 10 sec/45 m).

The single point and correlation statistics from the 623 LWC and r[eff] fields are used to generate 100 2D fields (512 x 50 pixels) and 25 3D fields (512 x 512 x 50 pixels). The LWC threshold for making the binary field for the correlation matrix is 0.01 g/m^3. Figure 1 shows the first eight stochastic 2D LWC fields. The cloud fraction and peak LWC varies markedly from field to field. Figure 2 shows the optical depth derived from the LWC and r[eff] of one stochastic 3D field.

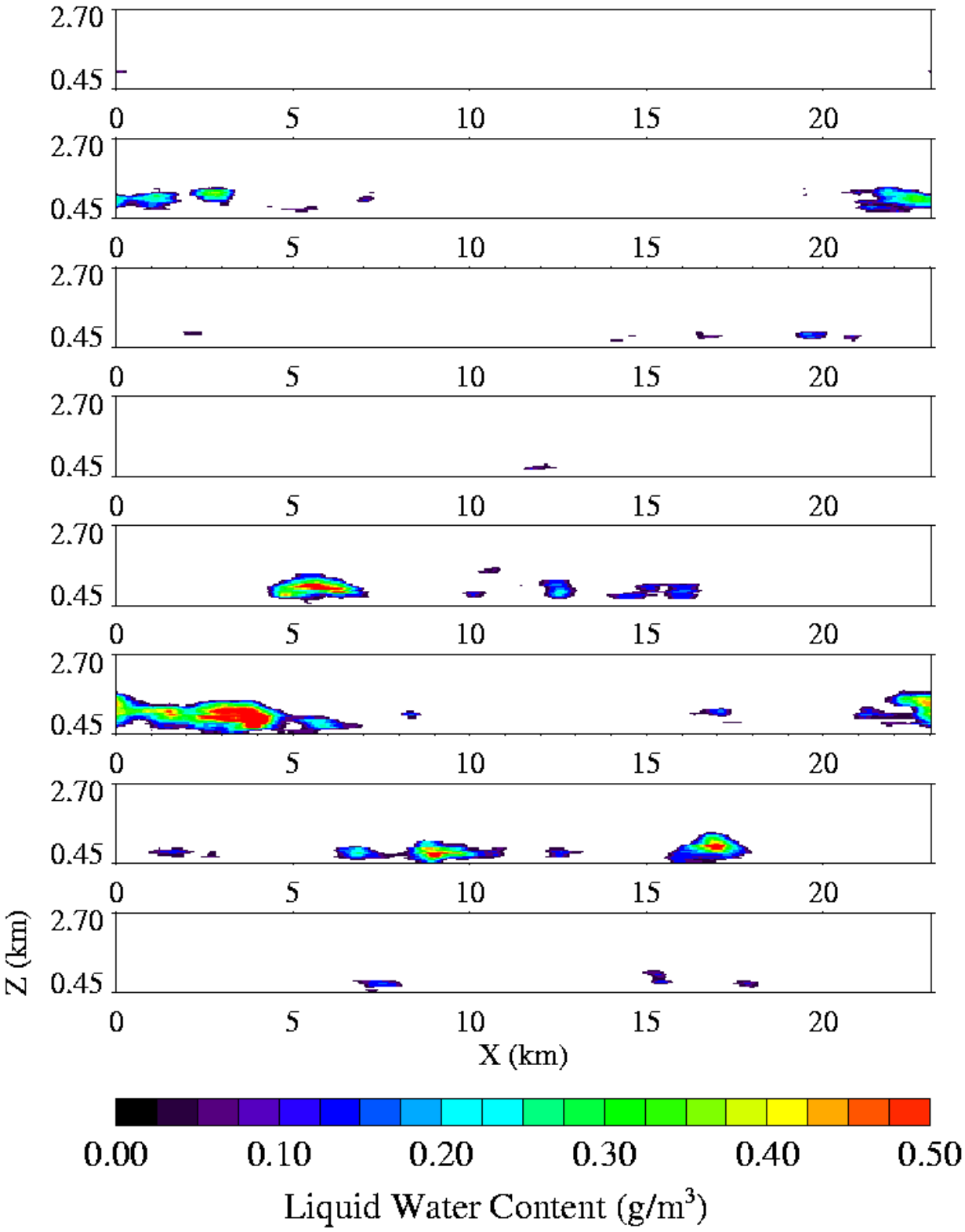

Figure 1. Eight of the stochastically generated 2D LWC fields.

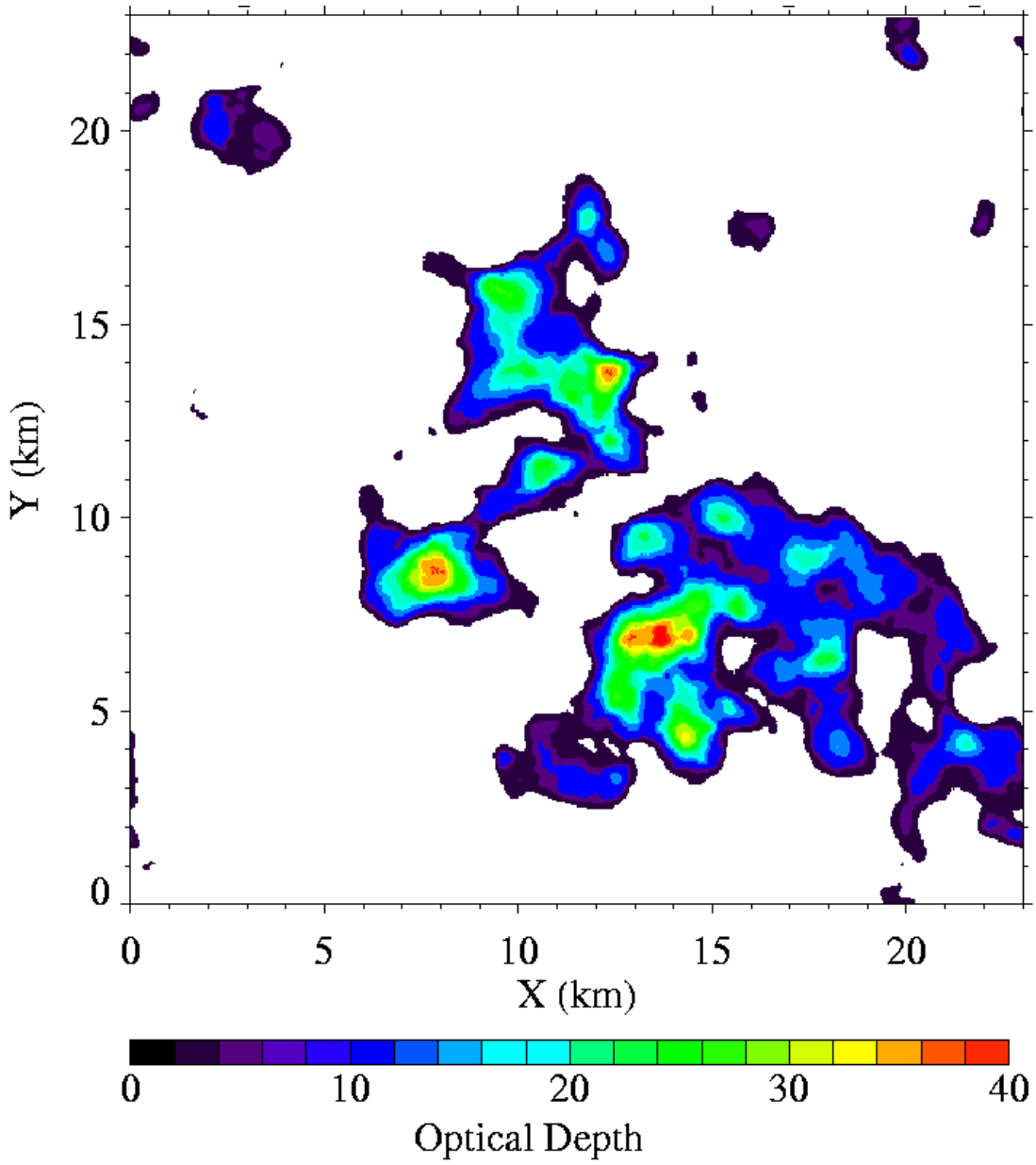

Figure 2. Example optical depth image from a stochastically generated 3D cloud field.

One way to assess the faithfulness of the stochastic cloud fields is to compare simple cloud statistics for the observed and stochastic fields. The most important cloud property for radiative transfer is the optical depth distribution which is shown in Figure 3. Here the threshold for a cloud is an optical depth of 1 and two range gates in thickness. The 2D and 3D stochastic cloud fractions are very close to the observed fraction of 18 percent, and the optical depth distributions are also quite close. The cloud geometrical thickness and width distributions, which are important for the horizontal radiative transfer effect, are compared in Figure 4. The stochastic thickness distributions agree well with the observed one. The 3D stochastic cloud width distribution is quite close to the observed one, but the 2D stochastic distribution has more clouds with width from 0.5 - 2.0 km than observed.

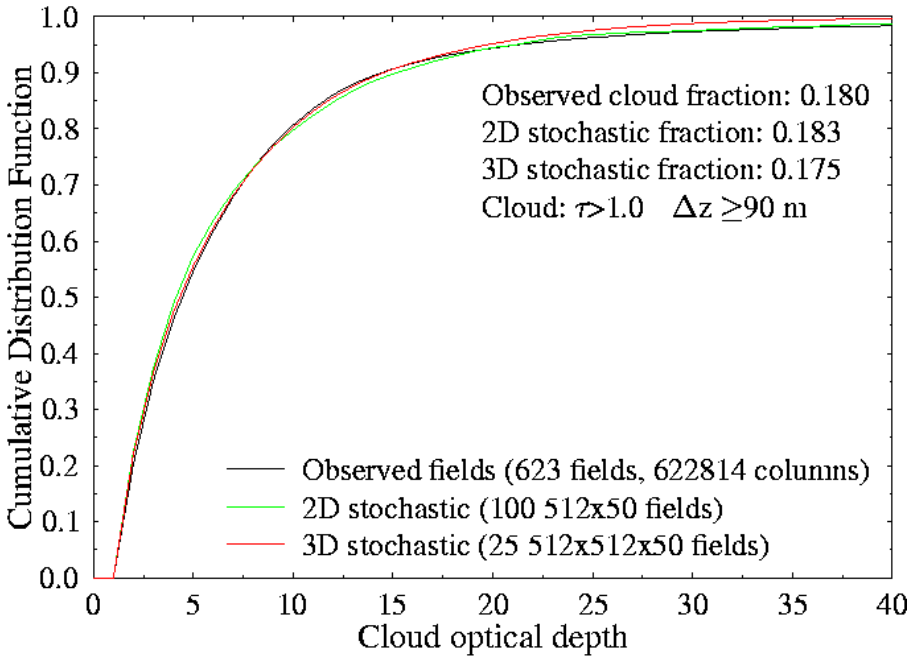

Figure 3. The observed and stochastic cloud optical depth distributions.

Radiative Transfer Modeling and Results

Broadband solar radiative transfer simulations are performed in the observed 2D cloud fields input to the stochastic generation algorithm and in the 2D and 3D stochastic cloud fields. Each of these simulations is done with plane-parallel (PP), independent pixel (IP), and 3D radiative transfer. The domain average broadband reflected and column absorbed fluxes are compared. The purposes are to determine 1) if the 2D stochastic fields are radiatively equivalent to the observed 2D fields, 2) the size of the 1D heterogeneity effect (PP-IP fluxes), and 3) the size of the horizontal transfer effect (IP-3D).

Broadband solar radiative transfer is calculated with a maximal cross section forward Monte Carlo code. Molecular absorption is included with the Fu and Liou (1992) band correlated k-distribution; five bands from 0.2 - 3.5 micron are used. A mean atmospheric sounding for convectively suppressed conditions in the Tropical West Pacific is input to the k-distribution. The cloud droplet optical properties are calculated with Mie theory for the liquid water content and effective radius fields assuming a gamma droplet size distribution with 0.1 effective variance. Fluxes are calculated for 5 solar zenith angles (SZAs) (0^{circ}, 27^{circ}, 45^{circ}, 56^{circ}, 63^{circ}) and a daytime average (average from sunrise to sunset with the Sun overhead at noon). The solar azimuth is fixed in the X-Z plane. A 5 percent Lambertian surface albedo is used for all wavelengths. The number of photons spread across the 5 bands is 1×10^5 for each of the 623 observed 2D fields, 3×10^5 for each of the 100 2D stochastic fields, and 1×10^6 for each of the 25 3D stochastic fields. Since the purpose of the computation is a relative comparison, very high accuracy in the k-distribution and other radiative transfer assumptions is not required.

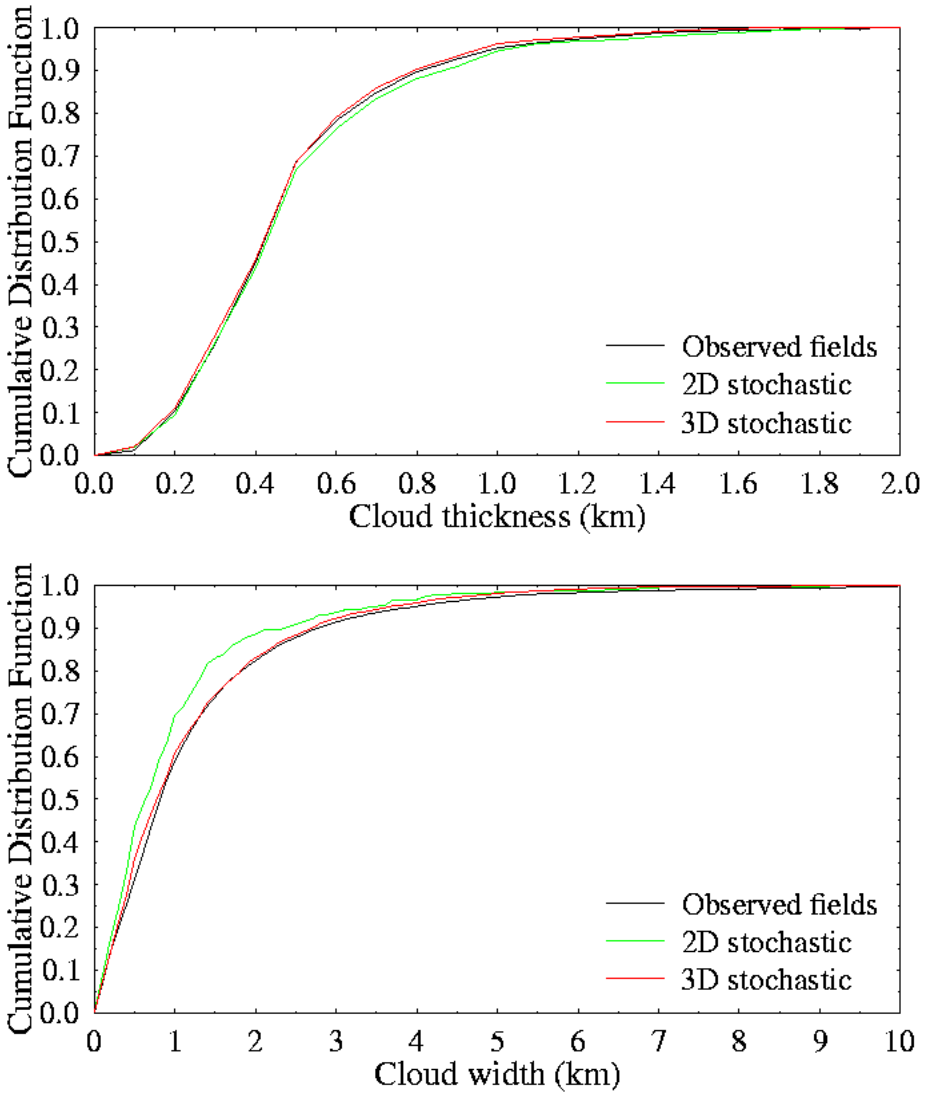

Figure 4. The observed and stochastic cloud thickness (top) and cloud width distributions.

The mean reflected fluxes over all the observed and stochastic 2D fields as a function of SZA are shown in Figure 5. The error bars indicate the standard deviation of the mean from scene-to-scene variation. The radiative forcing of these clouds is significant: the day time average reflected flux difference between clear and cloudy for the observed fields is 124 - 89 = 35 W/m^2. The reflected flux for the 2D stochastic fields agrees with the observed fields to well within the error bars.

The 1D heterogeneity error, which is the difference between plane-parallel and independent pixel fluxes, is shown in Figure 6a. There is good agreement in the PP-IP reflected and absorbed fluxes between the observed and stochastic fields. The uncertainty shown in the error bars is due to the scene variability and is not independent for the different SZAs; hence, the reflected PP-IP flux differences for the 2D stochastic fields is not statistically different from that for the observed fields. The 1D heterogeneity error is important for the Nauru cumulus clouds. For the observed fields the daytime average PP-IP difference in reflected flux is 5.8 W/m^2, though it is only 1.0 W/m^2 in absorbed flux.

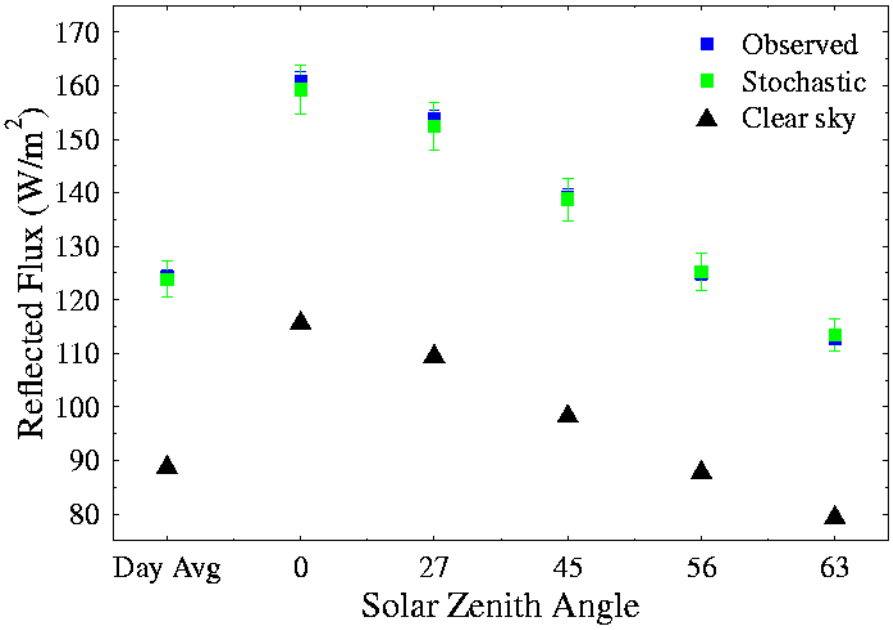

Figure 5. Broadband solar reflected fluxes from the observed 2D fields, the stochastic 2D fields, and clear sky.

The difference between the IP and 3D reflected fluxes, which is a measure of the horizontal transport or 3D radiative effect, is shown in Figure 6b. The reflected flux IP error of the 2D stochastic fields agrees within the error bars with that for the observed fields. The reflected flux IP error of the 3D stochastic fields is significantly larger than that for the 2D fields only for low sun angle. The daytime average reflected flux IP error for the 2D observed fields is -0.24 W/m^2, while for the 3D stochastic fields it is 0.17 W/m^2. The daytime averaged absorbed flux IP error is about -0.35 W/m^2 for the observed and stochastic fields. The horizontal transport effects are small for these fields because the cumulus clouds are small (mean thickness is 0.47 km, mean width is 1.3 km) and have low optical depth (mean is 7.2).

Conclusions

This study attempts to determine how important 3D solar radiative transfer effects are in small marine tropical cumulus fields observed with ARM remote sensing instruments at Nauru. A “data generalization” stochastic cloud generation algorithm is developed to simulate 3D fields of liquid water content (LWC) and effective radius (r_{eff}) from statistics derived from time-height cross sections. The stochastic cloud model generates fields with the correct histogram of LWC and r_{eff} and with the observed correlation function for the binary cloud mask field.

LWC and r_{eff} profiles for nonprecipitating cumulus clouds are derived from Nauru MMCR and MWR time series with the Bayesian retrieval algorithm of McFarlane et al. (2001b). Three months of data yield 623 segments with lengths from 1.5 to 3.0 hours (over 620,000 columns). These are converted to X-Z fields using advection speeds obtained from the NOAA 915 MHz wind profiler. The observed fields are input to the stochastic generation algorithm to produce 100 2D (512 x 50) fields and 25 3D (512 x 512 x 50) fields with 45 m resolution. The probability distributions of cloud optical depth, geometric thickness, and horizontal size for the stochastic fields agree well with the observed distributions.

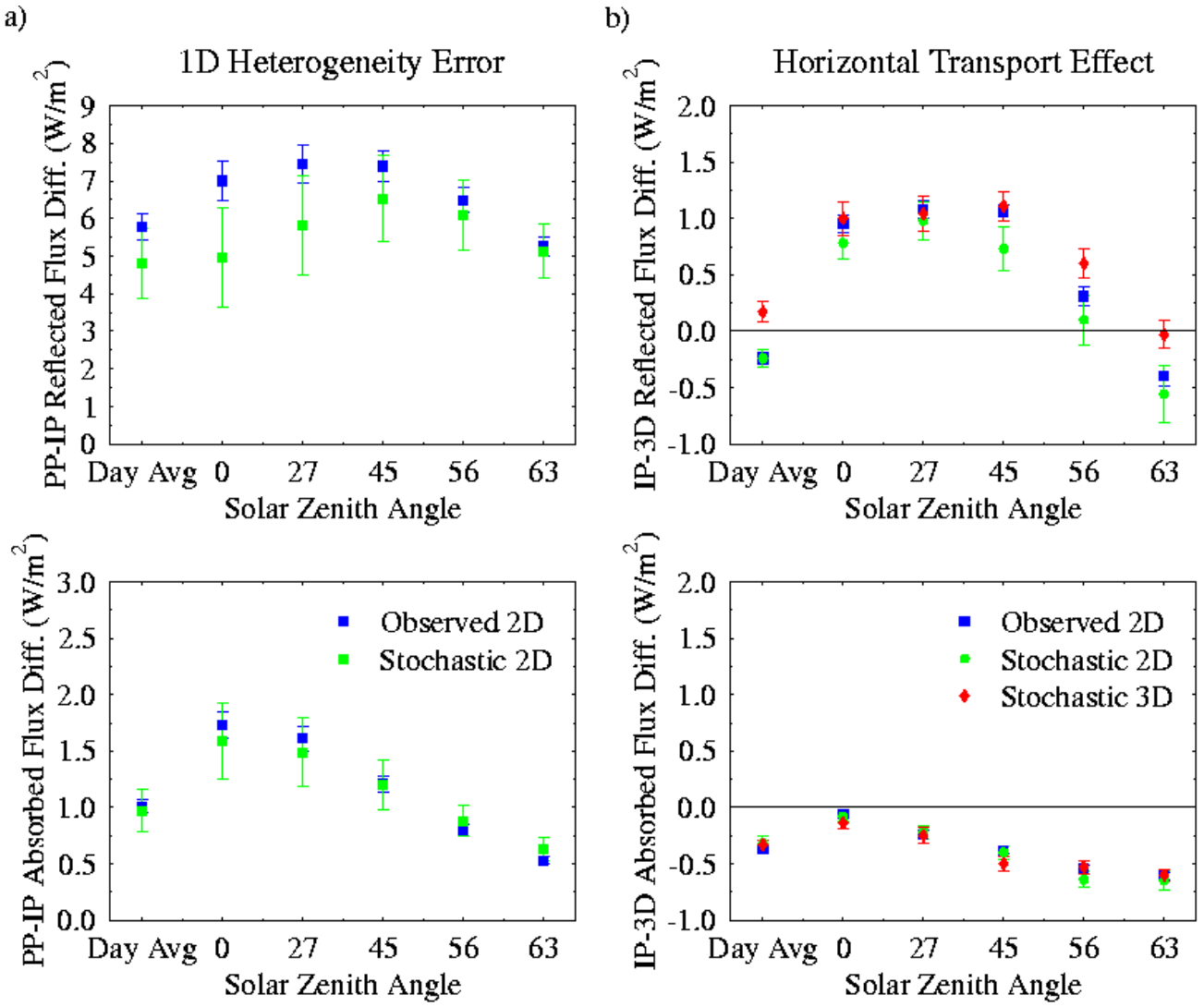

Figure 6. (a) Difference between plane-parallel and independent pixel broadband solar reflected and column absorbed fluxes for the observed and stochastic 2D fields (b) Difference between independent pixel and 3D broadband solar reflected and absorbed fluxes for the observed and stochastic 2D and 3D fields.

Broadband solar radiative transfer is simulated in the observed and stochastic cloud fields with plane-parallel (PP), independent pixel (IP), and 3D transfer. The reflected and column absorbed flux differences (i.e. PP-IP and IP-3D) from the 2D stochastic fields agree fairly well with those from the observed fields. This implies that the stochastic algorithm is generating radiatively equivalent cloud fields. The observed cloud fields have a substantial radiative forcing, reflecting 35 W/m^2 more than clear sky. The mean 1D heterogeneity effect (PP-IP) in reflected flux is significant (nearly 6 W/m^2 for the daytime average in the observed fields). The mean horizontal transport effect (IP-3D) is small at 0.17 W/m^2 for reflected flux and -0.33 W/m^2 in absorbed flux for the daytime mean in the stochastic 3D fields.

These results are from a large sample of nonprecipitating cumulus clouds that we expect is representative of the tropical marine environment in convectively suppressed conditions. The Nauru island effect may overstate the cloudiness somewhat, and we have ignored the effects of overlying cirrus clouds. This study found that the 1D heterogeneity effect is significant, which reinforces previous work indicating that general circulation model (GCM) cloud radiation parameterizations should take into account subgrid scale optical depth variability using methods based on the independent pixel approximation. Fair weather cumulus are very prevalent at Nauru, so the finite cloud or horizontal transfer effect might be expected to be important. This study suggests, however, that the horizontal transfer effect is small, which is consistent with another study of small marine tropical cumulus made with a different methodology (Benner and Evans 2001). This implies that GCM cloud radiation parameterizations can probably ignore net horizontal transport, and use independent pixel based parameterizations, for these types of clouds. We note, however, that the horizontal transfer effect can be substantial in particular scenes that have a high fraction of geometrically and optically thicker clouds.

Acknowledgments

The authors thank the NOAA Aeronomy Lab (Tropical Dynamics and Climate Group, Dr. Kenneth S. Gage, Program Leader) for the wind profiler data and the ARM archive for the rest of the Nauru data used. Financial support was provided by the Environmental Sciences Division of the U.S Department of Energy (under grant DE-A1005-90ER61069 to the NASA Goddard Space Flight Center) as part of the ARM program.

Corresponding Author

Frank Evans, evans@nit.colorado.edu, (303) 492-4994

References

Barker, H. W., and J. A. Davies, 1992: Solar radiative fluxes for stochastic, scale-invariant broken cloud fields. *J. Atmos. Sci*., **49**, 1115-1126.

Barker, H. W., J.-J. Morcrette, and G. D. Alexander, 1998: Broadband solar fluxes and heating rates for atmospheres with 3D broken clouds. *Q. J. R. Meteorol. Soc*., **124**, 1245-1271.

Benner, T. C., and K. F. Evans, 2001: Three-dimensional solar radiative transfer in small tropical cumulus fields derived from high-resolution imagery. *J. Geophys. Res*. (in press).
Cahalan, R. F., W. Ridgeway, W. J. Wiscombe, T. L. Bell, and J. B. Snider, 1994: The albedo of fractal stratocumulus clouds. *J. Atmos. Sci*., **51**, 2434-2455.

Fu, Q., and K. N. Liou, 1992: On the correlated k-distribution method for radiative transfer in nonhomogeneous atmospheres. *J. Atmos. Sci*., **49**, 2139-2156.

McFarlane, S. A., K. F. Evans, and A. A. Ackerman, 2001a: Liquid Water Cloud Retrievals: A Bayesian Approach. In *Proceedings of the Eleventh Atmospheric Radiation Measurement (ARM) Science Team Meeting.* Available URL: http://www.arm.gov/docs/documents/technical/conf_0103/.....pdf

McFarlane, S. A., K. F. Evans, and A. S. Ackerman, 2001b: A Bayesian Algorithm for the Retrieval of Liquid Water Cloud Properties from Microwave Radiometer and Millimeter Radar Data. Submitted to *J. Geophys. Res*.

Popescu, R., G. Deodatis, and J. H. Prevost, 1997: Simulation of homogeneous nonGaussian stochastic vector fields. *Prob. Engng. Mech.*, **13**, 1-13.

Varnai, T., and R. Davies, 1999: Effects of cloud heterogeneities on shortwave radiation: Comparison of cloud top variability and internal heterogeneity. *J. Atmos. Sci*., **56**, 4206-4224.

Welch, R. M., and B.A. Wielicki, 1984: Stratocumulus cloud field reflected fluxes: The effect of cloud shape. *J. Atmos. Sci*., **21**, 3086-3103.